Accepted Manuscript

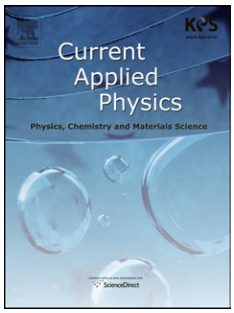

The energy transfer mechanism in Ce,Tb co-doped LaF_3 nanoparticles

H.A.A. Seed Ahmed, O.M. Ntwaeaborwa, R.E. Kroon

PII: S1567-1739(13)00142-9

DOI: 10.1016/j.cap.2013.03.021

Reference: CAP 3273

To appear in: *Current Applied Physics*

Received Date: 6 February 2013

Revised Date: 22 March 2013

Accepted Date: 25 March 2013

Please cite this article as: H.A.A.S. Ahmed, O.M. Ntwaeaborwa, R.E. Kroon, The energy transfer mechanism in Ce,Tb co-doped LaF_3 nanoparticles, *Current Applied Physics* (2013), doi: 10.1016/j.cap.2013.03.021.

The energy transfer mechanism in Ce,Tb co-doped LaF_3 nanoparticles

H.A.A. Seed Ahmed[a,b], O.M. Ntwaeaborwa[a] and R.E. Kroon[a,*]

[a]*Department of Physics, University of the Free State, Bloemfontein, South Africa*

[b]*Department of Physics, University of Khartoum, Khartoum, Sudan*

[*]***Corresponding Author.*** Email: KroonRE@ufs.ac.za Tel.: +27 514012884 Fax: +27 514013507 Address: Department of Physics, IB51, University of the Free State, Box 339, Bloemfontein 9300, South Africa.

Abstract: LaF_3 pure host, LaF_3:Ce, LaF_3:Tb as well as LaF_3:Ce,Tb phosphors were synthesized by the hydrothermal method. X-ray diffraction measurements were in good agreement with the standard data of LaF_3 from JCPDS card No. 32-0483 and indicated that the material was nanocrystalline with an average particle size of about 36 nm. Photoluminescence spectra of co-doped samples revealed that the Ce^{3+} emission was quenched while Tb^{3+} emission was enhanced, implying that energy was transferred from Ce^{3+} (the donor) to Tb^{3+} (the acceptor) in this system. The luminescence intensities and lifetimes of the donor for different concentrations of the acceptor were fitted to theoretical models in order to investigate the energy transfer mechanism. The quadrupole-quadrupole and exchange interaction mechanisms gave the best fit between the experimental data and the theoretical curves. The effective average Bohr radius from the fit to the exchange model is 0.095 nm. Since this is close to the ionic radii of the Ce^{3+} and Tb^{3+} ions, it suggests that the exchange interaction mechanism contributes to the energy transfer.

Keywords: Energy transfer; Lanthanum fluoride; Cerium; Terbium; Exchange interaction

1. Introduction

Developing efficient luminescent materials for application in modern technologies has attracted much interest in the last five decades. One way of enhancing the luminescence efficiency of these materials is through energy transfer between a donor and an acceptor, which are in most cases lanthanide ions. Among these lanthanide ions, Ce^{3+} has emerged as an excellent donor due to its allowed f-d absorption and its broad emission band which can easily overlap an acceptor absorption band, resulting in energy transfer to the acceptor. On the other hand, the bright green emission of Tb^{3+} makes this ion a popular acceptor of the lanthanide group. Lanthanum fluoride (LaF_3) is considered to be an ideal host material due to its superior thermal and environmental stability, as well as its low vibrational energy (~350 cm^{-1}) which minimizes non-radiative phonon-assisted quenching of the excited states of the dopant ions [1]. During the past decade there have been a significant number of reports focussing on nanoparticles with the specific composition $La_{0.4}F_3$: $Ce_{0.45}$,$Tb_{0.15}$ [2-8]. The composition $La_{0.8}F_3$:$Ce_{0.15}Tb_{0.05}$ has also been considered [9], while recently the properties of lanthanum fluoride nanocrystals produced using the hydrothermal method with varying amounts of Ce and Tb have been reported [1]. The quantum efficiency of these phosphors has been an important consideration, and although the energy transfer from Ce to Tb is evident from the previous reports, the mechanism for the energy transfer has not been reported and remains an interesting topic. A recent report states that the critical transfer distance for energy transfer from Ce to Tb has been estimated to be ~ 0.5 nm in LaF_3 [1], but this calculation was actually made for $Ce_{0.85}Tb_{0.15}F_3$ (containing no La) and assumes that energy transfer occurs via the dipole-dipole interaction mechanism [10]. In this study, the mechanism responsible for the energy transfer between Ce and Tb in LaF_3 was investigated by fitting both the luminescence intensity and the lifetime of the donor (Ce) as a function of the acceptor (Tb) concentration to the Inokuti and Hirayama theoretical models [11].

2. Materials and Methods

LaF_3 pure host, LaF_3:Ce, LaF_3:Tb as well as co-doped LaF_3:Ce,Tb phosphors were synthesized by the hydrothermal method. $La(NO_3)_3.6H_2O$ and NaF were used as starting materials and $Ce(NO_3)_3.6H_2O$ and $Tb(NO_3)_3.6H_2O$ were added for doping. Cetyltrimethylammonium bromide $C_{19}H_{42}BrN$ (CTAB) served as a surfactant to control the particle size. Each prepared sample

contained 5 mmol of the lanthanide ions (including dopants), 15 mmol of NaF and 1 mmol of CTAB. The nitrates, dissolved in 30 ml of water, were added to the CTAB in 10 ml of water. After stirring for 20 min, NaF dissolved in 10 ml of water was added drop by drop. After further stirring for 40 min, the mixture was transferred into a 125 ml autoclave lined with teflon and heated at 150°C for 12 h. The product was collected by centrifugation and washed first with water, and then with ethanol, each three times. The powder was finally dried in an oven at 80°C. By repeated dilution of a terbium nitrate solution, a series of LaF_3:Ce(1 mol%),Tb(x mol%) where x = 20, 10, 5, 2, 1, 0.5, 0.2, 0.1, 0.05 was prepared to analyse the mechanism of energy transfer between Ce and Tb ions. The structure of the prepared samples was characterised by X-ray diffraction (XRD) using a Bruker D8 diffractometer. Auger spectra and scanning electron microscopy (SEM) images were collected with a PHI 700 Scanning Auger Nanoprobe. Photoluminescence (PL) spectra were obtained with a Cary Eclipse fluorescence spectrophotometer. Luminescence decay curves were recorded using the SUPERLUMI station [12] at HASYLAB, DESY using synchrotron radiation with an Acton Research Corporation SpectraPro 300i spectrometer and Hamamatsu R6358P photomultiplier. All measurements were carried out at room temperature.

3. Results and discussion

Figure 1 shows the XRD patterns of undoped and doped LaF_3, together with the standard data for LaF_3 from JCPDS card No. 32-0483. The patterns for samples doped with 5 mol% of either Ce or Tb are similar to that of the pure host, showing that the Ce and Tb ions did not affect the structure and were well dispersed in the LaF_3 lattice. The heavily doped LaF_3:Ce(1%),Tb(20%) sample shows a slight shift of the diffraction peaks toward greater angles, implying that the lattice parameter has decreased, which is reasonable in terms of the smaller Tb ionic radius (0.0923 nm) compared to the La ions (0.1061 nm) that are substituted [6]. The particle size was estimated from the Scherrer [13] equation $\frac{K\lambda}{\beta\cos\theta}$ where K is the shape factor (0.9), λ is the wavelength and β is the FWHM of the x-ray peak at the Bragg angle θ (corrected for the instrument response). The average particle size of the undoped LaF_3 nanoparticles was 36 nm. For the doped samples the x-ray peaks were slightly wider than those of the undoped sample, but this can be explained by impurity broadening instead of a decrease in particle size.

Figure 2 shows the PL excitation and emission spectra for the LaF_3:Ce(1%). The excitation spectrum has a broad peak with a maximum at 247 nm corresponding to the 4f-5d absorption band of the Ce^{3+} ions. The broad emission spectrum exhibits two peaks centred at 287 and 301 nm which are attributed to the transitions from the lowest 5d excited state to the 4f ($^2F_{7/2}$ and $^2F_{5/2}$) ground state. Both the excitation and emission spectra are in agreement with reported data [14]. Excitation and emission spectra for LaF_3:Tb(5%) are shown in Figure 3. The excitation spectrum was recorded while monitoring the 542 nm green emission of Tb^{3+} ions. Nine absorption bands are found to correspond to f-f transitions of Tb^{3+}, from the $^7F_6$ ground state to: $^5I_7$ at 272 nm; $^5I_8$,$^5F_5$ at 284 nm; $^5H_6$ at 303 nm; $^5H_7$ at 318 nm; $^5D_1$ at 326 nm; $^5L_8$ at 342nm; $^5D_2$,$^5L_9$ at 352 nm; $^5L_{10}$ at 370 nm and $^5D_3$,$^5G_6$ at 379 nm [15]. Although Wang *et al.* [1] state that 4f-5d absorption bands of Tb^{3+} ions in LaF_3 occur from 250–280 nm, the lowest energy f-d absorption actually occurs near 200 nm [16]. The absorption band at 247 nm does not appear to be due to f-f or f-d absorption of Tb^{3+} and is most likely caused by very small amounts of Ce^{3+} impurity (the wavelength matches the f-d absorption of Ce in Figure 2) which could come from the porous teflon liner used for sample preparation with other samples containing Ce. The emission spectrum obtained from the Tb doped samples by exciting with 352 nm showed the characteristic green emission bands attributed to the $^5D_4$-^7F_J transitions (J=6,5,4,3) of Tb^{3+}, with the dominant green band at 542 nm.

Figure 4 shows the PL emission spectrum of the LaF_3:Ce(1%),Tb(5%) co-doped sample excited at 247 nm, compared to the emission spectra for the singly doped samples. The Ce emission in the co-doped sample was quenched and an enhancement of the Tb emission was observed. This can be attributed to energy transfer from the Ce^{3+} ions to Tb^{3+} ions. Figure 5 shows the overlap of the emission spectrum of LaF_3:Ce(1%) and the excitation spectrum of LaF_3:Tb(5%). The Ce emission overlaps several of the Tb f-f excitation bands, which is the essential condition for energy transfer to occur (without the need for phonons). The Tb excitation spectrum of the co-doped sample monitored at 542 nm (see Figure 5) showed a prominent peak at 247 nm, corresponding to Ce^{3+} f-d absorption, and relatively weak peaks associated with the Tb f-f excitation bands. To investigate the influence of the Ce concentration on the emission intensity from Tb in the co-doped samples, the concentration of Tb^{3+} ions was kept constant at 5 mol% and that of Ce^{3+} ions was varied from 0 up to 5 mol%. Figure 6 shows the relative intensity of Tb emission associated with the $^5D_4$-$^7F_5$ transition near 542 nm as a function of Ce concentration,

normalized with respect to the sample containing no Ce, i.e. the Tb single doped sample. It was found that the Tb emission increased as the Ce concentration increased up to 5 mol%. Although the concentration of Ce corresponding to a maximum was not reached, the rate of increase became small. It was decided to study the transfer mechanism using a fixed Ce concentration of 1 mol%, as a compromise between obtaining strong Tb emission through energy transfer, but not introducing more Ce than was necessary into the host. This also avoids possible interaction between Ce-Ce ions which may occur at high concentration, although it has been reported that practically no concentration quenching occurs in $La_{1-x}Ce_xF_3$, implying that energy migration between Ce ions is not significant, even for very high Ce concentrations [17].

The luminescence intensity and decay lifetime of the Ce donor as a function of the Tb acceptor concentration in co-doped LaF_3 samples were studied to determine the mechanism of the energy transfer from the Ce to the Tb ions. Inokuti and Hirayama [11] illustrated theoretically how the values of $\frac{I}{I_0}$ and $\frac{\tau_m}{\tau_0}$ depend on the acceptor concentration for different types of multipole as well as the exchange mechanism of energy transfer, where I_0 is the donor emission intensity in the absence of the acceptor and I is the corresponding intensity in the presence of an acceptor, and where

$$\tau_m = \int_0^\infty t\phi(t)dt \Big/ \int_0^\infty \phi(t)dt \tag{1}$$

is the mean decay time, $\phi(t)$ is the decay function after pulse excitation and τ_0 is the lifetime of the donor when the acceptor is absent. For multipole interactions the decay function is given by

$$\phi(t) = \exp\left[\frac{-t}{\tau_0} - \Gamma\left(1 - \frac{3}{s}\right)\frac{c}{c_0}\left(\frac{t}{\tau_0}\right)^{\frac{3}{s}}\right] \tag{2}$$

where s = 6, 8 or 10 for dipole-dipole, dipole-quadrupole and quadrupole-quadrupole interactions, c is the acceptor concentration and c_0 is some critical concentration at which the energy transfer rate from the donor equals its emission rate. The critical concentration can be related to a critical distance using $c_0 = \frac{3}{4\pi R_0^3}$. For the exchange interaction the decay function is given by

$$\phi(t) = \exp\left[\frac{-t}{\tau_0} - \gamma^{-\frac{3}{s}}\frac{c}{c_0}g\left(\frac{t}{\tau_0}e^{\gamma}\right)\right] \tag{3}$$

where $g\left(\frac{t}{\tau_0}e^{\gamma}\right)$ is a function that can be evaluated numerically [11]. The exchange constant γ is related to an effective Bohr interaction radius L between the ions by $\gamma = \frac{2R_0}{L}$. Values of $\frac{I}{I_0}$ for a fixed Ce donor concentration of 1 mol% and a range of Tb acceptor concentrations were measured with the Cary-Eclipse fluorescence spectrophotometer and the results are given in Figure 7 and Table 1. The quantum efficiency of the energy transfer is given by $\eta_T = 1 - \frac{I}{I_0}$ [11] and a value of 87% was obtained for LaF_3:Ce(1%),Tb(20%). The Ce donor lifetime curves were measured using synchrotron radiation at SUPERLUMI using photon counting with a photomultiplier tube detector, with an excitation wavelength of 247 nm. The time between bunches limited the measuring period to about 70 ns. The experimental curves were fitted to multi-exponential functions (3 exponentials were found to be adequate) which were convoluted with the stray light signal measured on the system, and the fitted multi-exponential curves were used to calculate the mean decay times τ_m. Figure 8 presents several of the processed lifetime decay curves. The decay curve for singly doped LaF:Ce 1 mol% was processed in the same way as for the co-doped samples, but with only a single-exponential function, and the lifetime was found to be 29 ns for the 287 nm emission and 31 ns for the 301 nm emission. These values are similar to the lifetime reported for smaller Ce-doped LaF_3 nanoparticles coated with undoped LaF_3 shells [18]. The decay time was slightly longer for the longer wavelength emission, as has been reported for Ce doped $NaCaPO_4$ [19].

Figure 9(a) shows the experimental data $\frac{I}{I_0}$ and $\frac{\tau_m}{\tau_0}$ associated with the peak at 287 nm (closed shape) and the peak at 301 nm (open shape) plotted against one another and compared to the theoretical curves expected for different types of multipole interactions, which were calculated using the method of Inokuti and Hirayama [11]. The results match what one may expect if the energy transfer occurs due to quadrupole-quadrupole interaction, and is not consistent with either dipole-dipole or dipole-quadrupole interactions. To determine the critical concentration c_0, least squares fits were made for the quadrupole-quadrupole interaction of $\frac{I}{I_0}$ against $\frac{c}{c_0}$ and $\frac{\tau_m}{\tau_0}$ against $\frac{c}{c_0}$ with c_0 as the fit parameter (Figure 9(b)), giving values of 8.58 and 9.77 mol%

respectively. These were averaged and the result was converted to a volume concentration (using a molar volume of 33 cm^3/mol for LaF_3), and used to calculate the critical distance R_0 of 0.52 nm. Despite the fact that this value is obtained on the basis of quadrupole-quadrupole interaction, its value is almost the same as that reported before using a calculation based on the dipole-dipole interaction [1,10]. The experimental data was also fitted to the exchange interaction model for energy transfer. For this model, in addition to C_0, the exchange constant Y is also a parameter. The experimental data of $\frac{I}{I_0}$ and $\frac{\tau_m}{\tau_0}$ were plotted against one another and compared to the theoretical curves of several values of Y as computed using the method of Inokuti and Hirayama [11]. The experimental data corresponds well to the exchange interaction for Y =11.6 (see Figure 10(a)). This value for Y was fixed and least squares fits of $\frac{I}{I_0}$ against $\frac{C}{C_0}$ and $\frac{\tau_m}{\tau_0}$ against $\frac{C}{C_0}$ with C_0 as the fit parameter were made for exchange model (Figure 10(b)) in order to determine the critical concentration C_0, giving values of 8.02 and 7.97 mol% respectively. The average critical concentration was used to calculate the critical distance R_0 of 0.55 nm, which is similar to that obtained for the quadrupole-quadrupole interactions. As pointed out by Nakazawa and Shionoya [20], it can be difficult to distinguish between the higher order multipole interactions and the exchange interaction by analysing the luminescence intensity and lifetime of the donor emission. To check if the exchange mechanism is feasible, the effective average Bohr radius L should be similar to the ionic radii of the interaction ions, i.e. 0.1 nm for the lanthanides. In the present case the values of R_0 and Y give an effective average Bohr radius L = 0.095 nm, which means the exchange interaction mechanism can contribute to the energy transfer between Ce and Tb, although quadrupole-quadrupole interaction cannot be eliminated.

Using a similar method to that in this study, Nakazawa and Shionoya [20] found that energy transfer between unlike lanthanide ions in calcium metaphosphate glass was governed by dipole-quadrupole interactions. However, cerium was not one of the dopants considered. Wang *et al.* [21] reported that the dipole-dipole interaction was responsible for energy transfer from Ce to Tb in $CaAl_2SiO_6$. To our knowledge, energy transfer from Ce to Tb has not been attributed to the quadrupole-quadrupole interaction before. This mechanism has been reported for energy transfer

from Eu to Pr in $K_5Li_2GdF_{10}$, although the exchange mechanism was not considered in that study [22]. In contrast to a recent report on Ce,Tb co-doped $LaPO_4$ nanoparticles [23] in which energy transfer is suggested to not affect the decay kinetics of the Ce emission, in this study changes in the Ce decay curves could be observed and correlated to energy transfer from Ce to Tb.

4. Conclusion

Ce and Tb have been successfully incorporated singly, as well as together, in LaF_3 nanoparticles via the hydrothermal method. The crystal structure of LaF_3 remained unchanged after being doped with Ce^{3+} and Tb^{3+} ions, with a slight decrease in the lattice parameter in the samples having a heavy dopant concentration. The estimated particle size was 36 nm. The excitation and emission spectra of the single doped samples are in a good agreement with the reported values. Energy transfer from Ce to Tb was achieved in the co-doped samples with a quantum efficiency for energy transfer around 87% for the LaF_3:Ce(1%),Tb(20%) sample. The data associated with the luminescence intensity and lifetime of the donor as a function of the acceptor concentration fitted well to the Inokuti and Hirayama nonradiative energy transfer models corresponding to the quadrupole-quadrupole mechanism and the exchange interaction mechanism. Due to the short effective average Bohr radius L calculated from the obtained fitted parameters, the exchange interaction could not be excluded and it may contribute to the energy transfer together with quadrupole-quadrupole interaction.

Acknowledgments

Measurements at DESY were made under project I-20110503 (R.E. Kroon) and the authors thank Aleksei Kotlov for assistance. O.M. Ntwaeaborwa and R.E. Kroon acknowledge the financial support from the South African National Research Foundation (NRF). R.E. Kroon also acknowledges financial assistance from the Faculty of Natural and Agricultural Sciences, University of the Free State.

References

[1] Q. Wang, Y. You, R.D. Ludescher, Y. Ju, J. Lumin. 130 (2010) 1076.

[2] J.W. Stouwdam, G.A. Hebbink, J. Huskens, F.C.J.M. van Veggel, Chem. Mater. 15 (2003) 4604.

[3] J.W. Stouwdam, F.C.J.M. van Veggel, Langmuir 20 (2004) 11763.

[4] F. Wang, Y. Zhang, X. Fan, M. Wang, J. Mater. Chem. 16 (2006) 1031.

[5] X. Zhu, Q. Zhang, Y. Li, H. Wang, J. Mater. Chem. 18 (2008) 5060.

[6] Y. Liu, W. Chen, S. Wang, A.G. Joly, S. Westcott, B.K. Woo, J. Appl. Phys. 103 (2008) 063105.

[7] M.Y. Xie, L. Yu, H. He, X.F. Yu, J. Solid State Chem. 182 (2009) 597.

[8] H. He, M.Y. Xie, Y. Ding, X.T. Yu, Appl. Surf. Sci. 255 (2009) 4623.

[9] T. Zhang, H. Guo, Y. Qiao Y, J. Lumin. 129 (2009) 861.

[10] Z.L. Wang, Z.W. Quan, P.Y. Jia, C.K. Lin, Y. Luo, Y. Chen, J. Fang, W. Zhou, C.J. O'Connor, J. Lin, Chem. Mater. 18 (2006) 2030.

[11] M. Inokuti, F. Hirayama, J. Chem. Phys. 43 (1965) 1978.

[12] G. Zimmerer, Rad. Meas. 42 (2007) 859.

[13] P. Scherrer, Göttinger Nachrichten Math. Phys. 2 (1918) 98.

[14] C. Pedrini, B. Moine, J.C. Gacon, B. Jacquier, J. Phys.: Condens. Matter 4 (1992) 5461.

[15] W.T. Carnall, H. Crosswhite, H.M. Crosswhite, Argonne National Laboratory Report ANL-78-XX-95 (1978).

[16] P. Dorenbos, J. Phys.: Condens. Matter 15 (2003) 6249.

[17] G. Blasse, A. Bril, J. Chem. Phys. 51 (1969) 3252.

[18] L.G. Jacobsohn, A. Toncelli, K.B. Sprinkle, C.J. Kucera, J. Ballato, J. Appl. Phys. 111 (2012) 074315.

[19] Y. Wang, J. Zhang, D. Hou, H. Liang, P. Dorenbos, S. Sun, Y. Tao, Opt. Mater. (Amsterdam, Neth.) 34 (2012) 1214.

[20] E. Nakazawa, S. Shionoya, J. Chem. Phys. 47 (1967) 3211.

[21] B. Wang, L. Sun, H. Ju, Solid State Comm. 150 (2010) 1460.

[22] P. Solarz, W.R. Romanowski, Radiat. Meas. 42 (2007) 759.

[23] V. Pankratov, A.I. Popov, S.A. Chernov, A. Zharkouskaya, C. Feldmann, Phys. Status Solidi B 247 (2010) 2252.

Figure captions

Figure 1. XRD pattern of (a) LaF_3, (b) LaF_3:Ce(5%), (c) LaF_3:Tb(5%), and (d) LaF_3:Ce(1%)Tb(20%). At the bottom is the standard data of LaF_3 from JCPDS card 32-0483.

Figure 2. Excitation and emission for the LaF_3:Ce(1%).

Figure 3. Excitation and emission spectra for LaF_3:Tb(5%). Labels for f-f transitions are from the $^7F_6$ ground state. The peak marked with (*) is attributed to small amounts of Ce impurity.

Figure 4. PL spectrum of the LaF_3:Ce(1%),Tb(5%) sample excited with 247 nm (dashed) compared with the PL spectra of LaF_3:Ce(1%) and LaF_3:Tb(5%) samples (solid).

Figure 5. The emission spectrum of LaF_3:Ce(1%) showing the overlap with the excitation spectrum of LaF_3:Tb(5%), and the Tb excitation spectrum of LaF_3:Ce(1%),Tb(5%).

Figure 6. Intensity of the Tb $^5D_4$-$^7F_5$ emission (λ = 542 nm) as a function of Ce co-doping concentration for LaF_3 containing 5 mol% Tb.

Figure 7. Intensity of Ce emission for a range (0%-20%) of Tb concentrations for co-doped LaF_3.

Figure 8. Ce lifetime data and fitted decay curves for LaF_3:Ce(1%),Tb(x%) where x is 0%, 5%, 10%, and 20%.

Figure 9. (a) Experimental data of $\frac{I}{I_0}$ vs $\frac{\tau_m}{\tau_0}$ (closed and open circle) fitted to the theoretical curves (solid lines) of dipole-dipole ($s = 6$), dipole-quadrupole ($s = 8$), and quadrupole-quadrupole ($s = 10$) interaction. (b) Experimental data of $\frac{I}{I_0}$ (closed and open square) vs $\frac{c}{c_0}$ and $\frac{\tau_m}{\tau_0}$ (closed and open triangle) vs $\frac{c}{c_0}$ fitted to the theoretical curves (solid lines) of the quadrupole-quadrupole interaction. Note that closed and open shapes correspond to the peaks at 287 nm and 301 nm respectively.

Figure 10. (a) Experimental data of $\frac{I}{I_0}$ vs $\frac{\tau_m}{\tau_0}$ (closed and open circle) fitted to the theoretical curves (solid lines) for the exchange interaction ($\gamma = 8, 10, 12$ **and** 14). The dashed line gives the best fit ($\gamma = 11.6$). (b) Experimental data of $\frac{I}{I_0}$ (closed and open square) vs $\frac{c}{c_0}$ and $\frac{\tau_m}{\tau_0}$ (closed and open triangle) vs $\frac{c}{c_0}$ fitted to the theoretical curves (solid lines) of exchange interaction. Note that closed and open shapes correspond to the peaks at 287 nm and 301 nm respectively.

Table 1 Luminescence intensity and lifetime for the donor Ce in LaF_3:Ce,Tb as a function of Tb acceptor.

Tb concentration (mol%)	Ce peak at 287 nm			Ce peak at 301 nm		
	$\frac{I}{I_0}$	τ_m (ns)	$\frac{\tau_m}{\tau_0}$	$\frac{I}{I_0}$	τ_m (ns)	$\frac{\tau_m}{\tau_0}$
0	1	29.23	1	1	30.94	1
0.0500	0.984	28.63	0.979	0.981	30.37	0.982
0.100	0.981	28.58	0.978	0.978	30.32	0.980
0.200	0.964	28.50	0.975	0.958	30.17	0.975
0.500	0.956	28.25	0.966	0.951	29.93	0.967
1.00	0.855	27.87	0.954	0.844	29.51	0.954
2.00	0.758	27.62	0.945	0.737	29.17	0.943
5.00	0.526	24.24	0.829	0.500	25.97	0.839
10.0	0.306	19.79	0.677	0.277	20.22	0.653
20.0	0.134	14.09	0.482	0.121	14.63	0.473

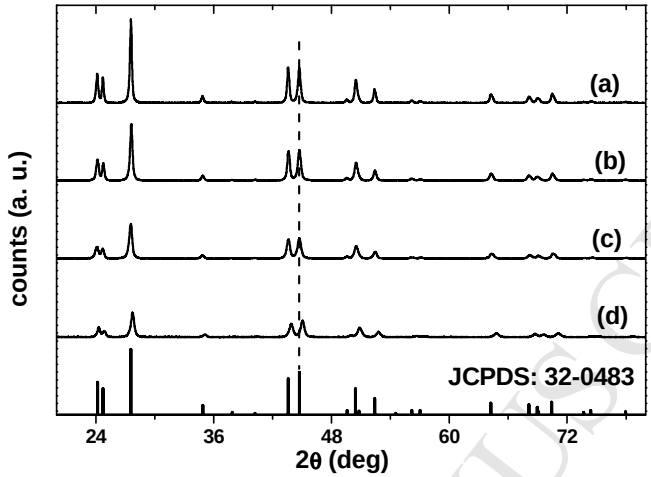

Figure 1

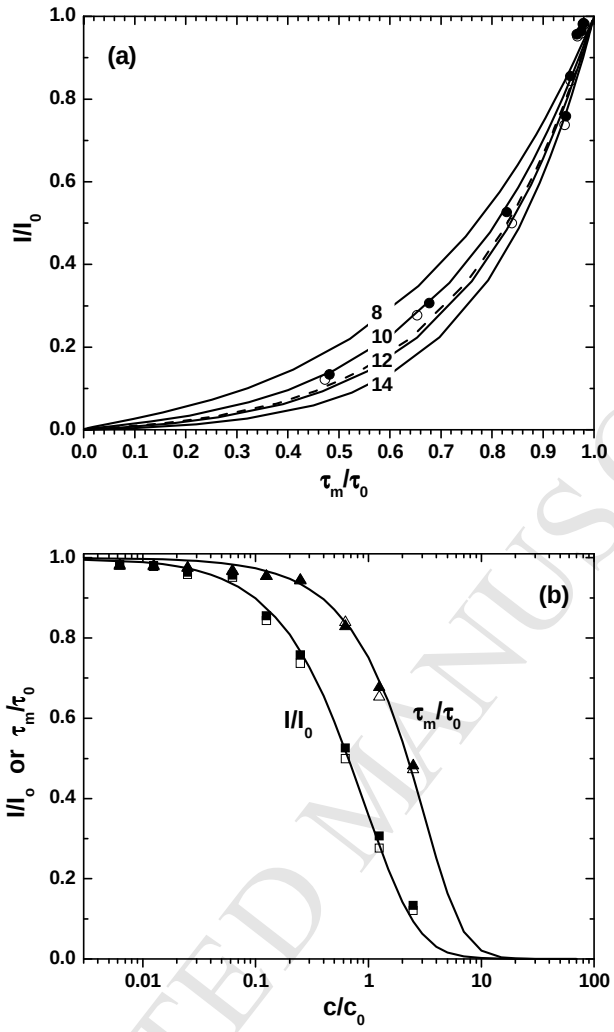

Figure 10

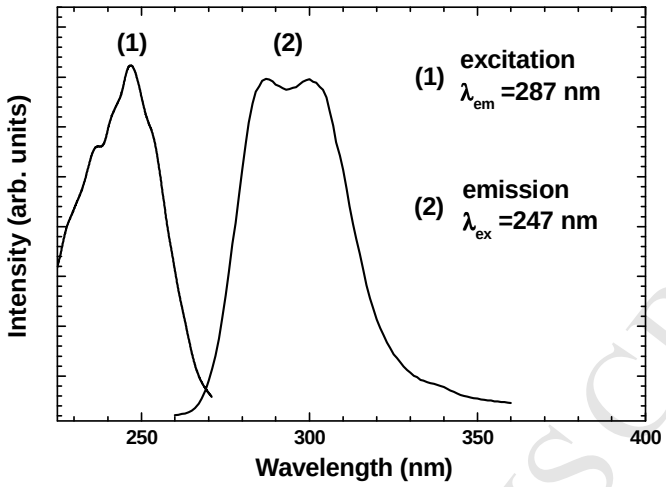

Figure 2

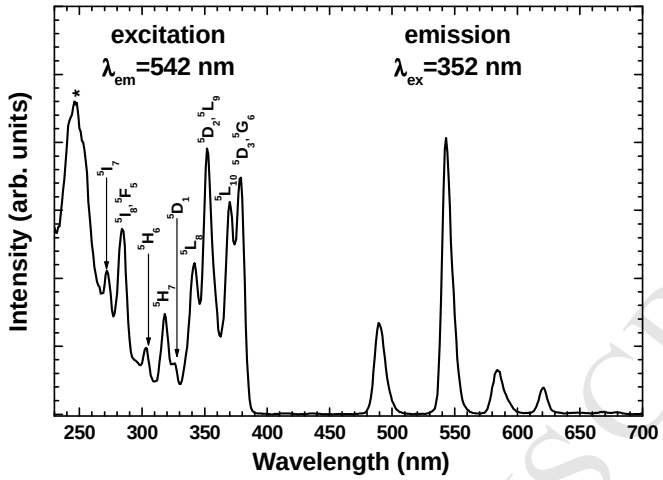

Figure 3

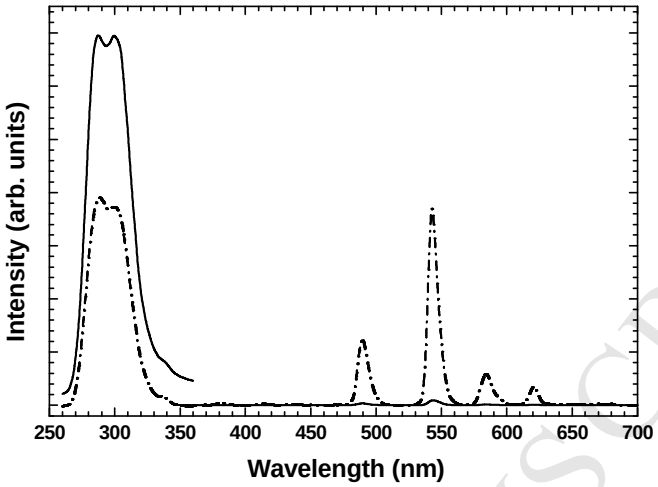

Figure 4

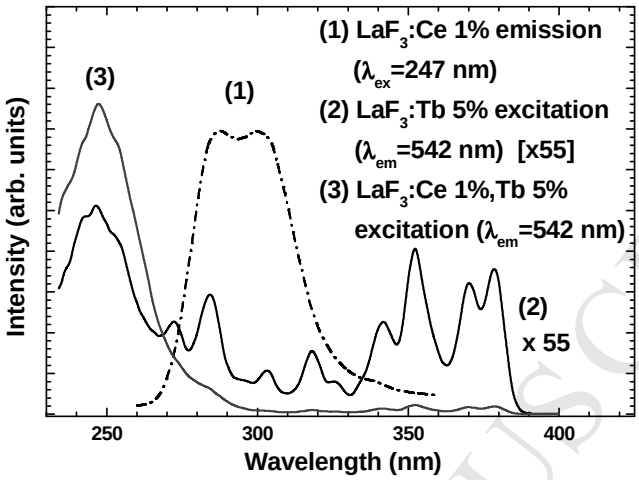

Figure 5

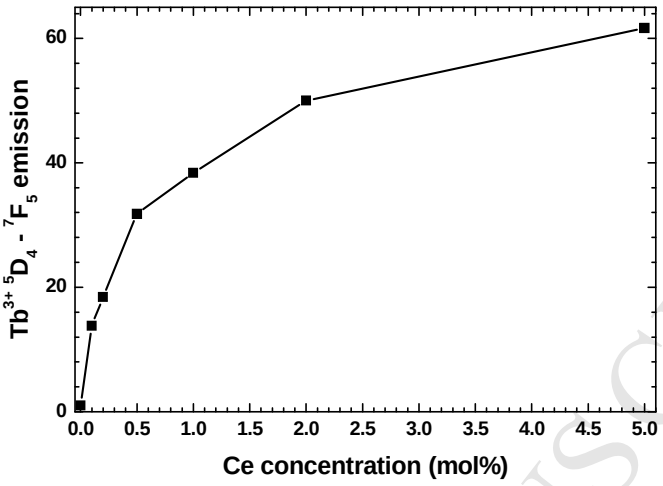

Figure 6

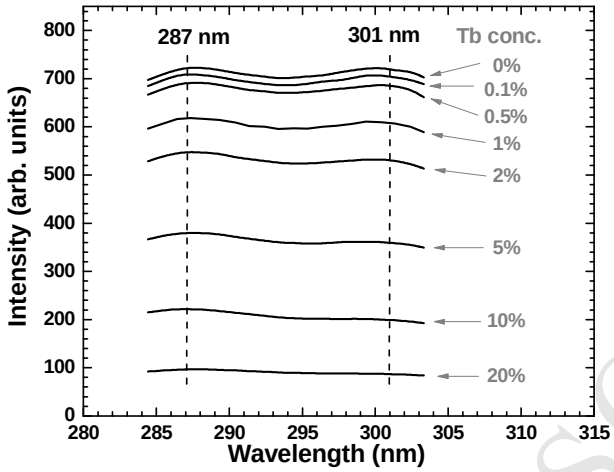

Figure 7

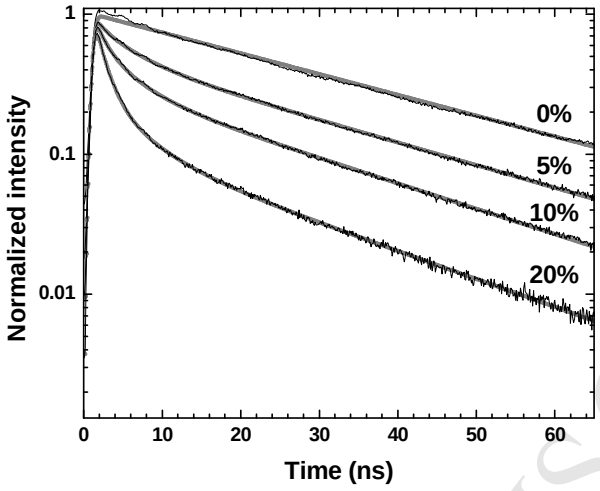

Figure 8

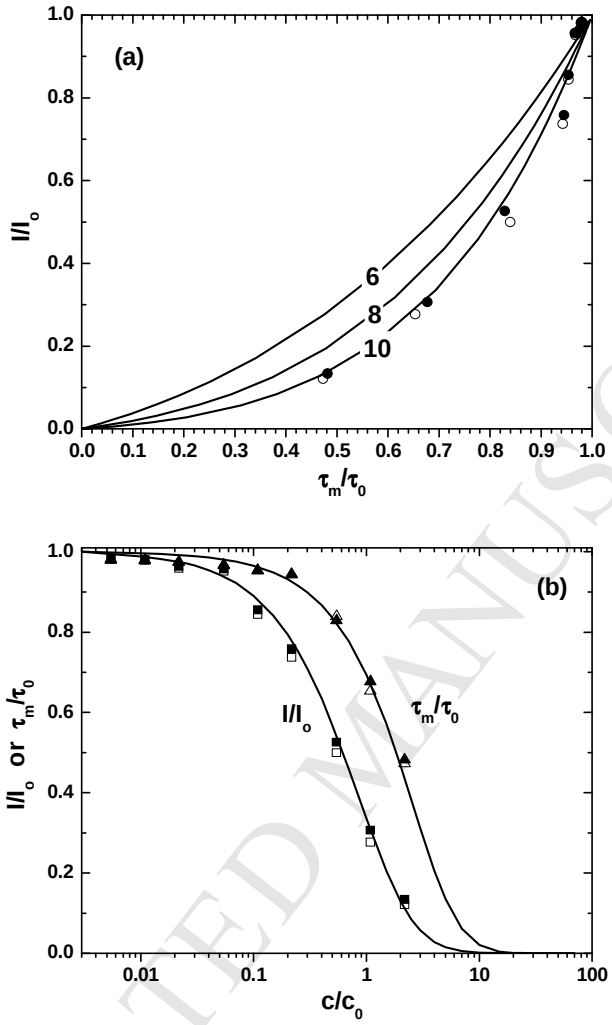

Figure 9

Highlights

- **Efficient luminescence from nanocrystalline LaF_3 doped with Ce or Tb using hydrothermal method**
- **Energy transfer from Ce to Tb occurs but a high concentrations of Tb is required to quench Ce emission**
- **Energy transfer is attributed to quadrupole-quadrupole and/or exchange mechanisms**